Aerosol and Air Quality Research

ORIGINAL RESEARCH
https://doi.org/10.4209/aaqr.210069

Influence of Meteorological Conditions and Fire Hotspots on $PM_{0.1}$ in Northern Thailand during Strong Haze Episodes and Carbonaceous Aerosol Characterization

Chaiyoth Sresawasd[1,2], Thaneeya Chetiyanukornkul[3], Phuchiwan Suriyawong[3], Surajit Tekasakul[4], Masami Furuuchi[5], Mitsuhiko Hata[5], Rachane Malinee[1,2], Perapong Tekasakul[1,6], Racha Dejchanchaiwong[1,7*]

[1] Air Pollution and Health Effect Research Center, Prince of Songkla University, Hat Yai, Songkhla 90110, Thailand
[2] Energy Technology Program, Faculty of Engineering, Prince of Songkla University, Hat Yai, Songkhla 90110, Thailand
[3] Department of Biology, Faculty of Science, Chiang Mai University, Mueang, Chiang Mai, 50200, Thailand
[4] Department of Chemistry, Faculty of Science, Prince of Songkla University, Hat Yai, Songkhla 90110, Thailand
[5] Faculty of Geoscience and Civil Engineering, Institute of Science and Engineering, Kanazawa University, Kakuma-machi, Kanazawa, Ishikawa 920-1192, Japan
[6] Department of Mechanical and Mechatronics Engineering, Faculty of Engineering, Prince of Songkla University, Hat Yai, Songkhla 90110, Thailand
[7] Department of Chemical Engineering, Faculty of Engineering, Prince of Songkla University, Hat Yai, Songkhla 90110, Thailand

ABSTRACT

Northern Thailand has long been severely affected by haze from biomass burning containing fine and ultrafine aerosols in the dry period. The carbonaceous $PM_{0.1}$ comprising elemental carbon (EC) and organic carbon (OC) collected during the haze and non-haze periods in Chiang Mai, Thailand was investigated. The $PM_{0.1}$ levels during the haze periods were about 3 times higher than the non-haze periods, a significant increase. $PM_{0.1}$ concentration was strongly correlated with atmospheric relative humidity and the number of forest fire hotspots. Carbonaceous aerosol characteristics in $PM_{0.1}$ were analyzed with the thermal/optical transmittance (TOT) method following the IMPROVE protocol. The concentrations of OC and EC, distribution of OC and EC and OC/EC ratios in $PM_{0.1}$ were evaluated. Average OC and EC mass concentrations in $PM_{0.1}$ were 6.8 $\pm$ 2.7 and 1.4 $\pm$ 0.5 μg m^{-3} during the haze periods, significantly higher than those during the non-haze periods; 1.9 $\pm$ 0.9 and 0.5 $\pm$ 0.2 μg m^{-3}. The OC/EC ratio increased linearly with the number of hotspots. This indicated significant contribution from biomass burning to the $PM_{0.1}$. This was strongly supported by the 48-hr backward trajectory simulation, that indicated both domestic and transboundary aerosol transports. Because both organic and elemental carbon are the light-absorbing carbonaceous aerosols, the increase during the haze periods contributed to regional air quality and climate. This study enhances the understanding of $PM_{0.1}$ behavior in Chiang Mai, Thailand, during the haze periods in upper southeast Asia.

Keywords: Ultrafine particles, Carbonaceous aerosols, Forest fire, Source identification, ASEAN haze

OPEN ACCESS

Received: March 27, 2021
Revised: July 13, 2021
Accepted: August 23, 2021

* **Corresponding Author:**
racha.d@psu.ac.th

Publisher:
Taiwan Association for Aerosol Research
ISSN: 1680-8584 print
ISSN: 2071-1409 online

1 INTRODUCTION

The current ambient air quality standard of particulate matters focuses on $PM_{2.5}$ mass concentrations. However, ultrafine particles or nanoparticles ($PM_{0.1}$) has recently become of more concern, because they are more carcinogenic and can cause greater health effect than larger particles due to larger surface area (Sharma and Balasubramanian, 2018; Ajdary *et al.*, 2018; Schraufnagel, 2020). Besides traveling deep into the lung mainly in the alveolar region (Schraufnagel, 2020), $PM_{0.1}$ can translocate from the cardiopulmonary system to the central nervous system by crossing the blood-brain barrier, and potentially cause brain damage (Cheng *et al.*, 2016; Jew *et al.*, 2019; Morris-Schaffer *et al.*, 2019; Hahad *et al.*, 2020; Potter *et al.*, 2021). A recent study in Thailand showed that $PM_{0.1}$ represented more than 5.7–14.8% of total suspended particulates (TSP) in atmospheric air (Chomanee *et al.*, 2020).

Southeast Asia (SEA) is strongly affected by atmospheric haze pollution (Wiriya *et al.*, 2013; Li and Shao, 2009; Pongpiachan *et al.*, 2014a; Pongpiachan *et al.*, 2015; Chuang *et al.*, 2016; Li *et al.*, 2016; Chomanee *et al.*, 2020; Dejchanchaiwong *et al.*, 2020; ChooChuay *et al.*, 2020a, b, c; Dejchanchaiwong and Tekasakul, 2021). In the upper SEA, the haze is observed during the first quarter of every year and studied, mostly in Thailand (Wiriya *et al.*, 2013, 2016; Thepnuan *et al.*, 2019; Pani *et al.*, 2019), but recently, air quality affected by PM_{10} and $PM_{2.5}$ was studied in Laos (Nguyen *et al.*, 2019), Myanmar (Sricharoenvech *et al.*, 2020) and Vietnam (Le, 2020). Previous investigations showed that aerosol particles in northern Thailand originated from biomass burning both transboundary and domestic sources (Wiriya *et al.*, 2013). Domestic sources of haze phenomena in northern Thailand were predominantly from forest fires, which occurred mostly in deciduous dipterocarp forest national parks, whereas the agricultural waste burning was minor. The total burnt area, in northern Thailand was about 1 Mha during Jan 1 to Apr 16, 2019: more than 90% of the burnt area was in the forest and only 5% in agricultural areas (GISTDA, 2020; Earthdata, 2020). Forest fires were triggered by human activities, including forest foraging (collecting wild plants and pursuing wild animals), land clearing, resource collection, accidents, land tenure conflicts, logging, etc. Forest fires in northern Thailand adversely affected the livelihood of people, leading to significant poverty.

Biomass burning is an important source of $PM_{0.1}$—accounting for more than 30% of the smoke particles (Hata *et al.*, 2014)—though the dominant size of PM from biomass burning was in accumulation mode particles ($PM_{0.5\text{-}1.0}$) (Tekasakul *et al.*, 2008; Hata *et al.*, 2014; Phairuang *et al.*, 2019; Dejchanchaiwong *et al.*, 2020; Chomanee *et al.*, 2020). Biomass burning emissions contain a significant number of carbonaceous aerosols, i.e., organic carbon (OC) and elemental carbon (EC), released into the atmosphere (Chow *et al.*, 2004; Chow *et al.*, 2005; Chow *et al.*, 2007; Chuang *et al.*, 2016; Lee *et al.*, 2016; Pani *et al.*, 2019). Carbon was a significant component of fine particles, accounting for 20–60% of $PM_{2.5}$ mass in urban areas (Phairuang *et al.*, 2019). Elemental carbon was the primary emission, generated from carbon fuel-based combustion. Organic carbon can be formed by direct emission and through secondary pathways (Chu *et al.*, 2005; Han *et al.*, 2009). Carbonaceous aerosols are formed from various emission sources. Hence, the OC/EC ratio is an important identifier of PM emission sources (Chu *et al.*, 2005; Pongpiachan *et al.*, 2014b; Han *et al.*, 2016; Haque *et al.*, 2019). Recently, Pani *et al.* (2019) reported that the OC and EC concentrations for $PM_{2.5}$ in Chiang Mai, Thailand, in March 2015 were OC 46.6 ± 19.0 μg m^{-3} (42.9 ± 5.0%) and EC 9.5 ± 4. μg m^{-3} (8.9 ± 2.7%). The OC/EC ratios for $PM_{2.5}$ ranged from 4.9 ± 1.7 to 5.6 ± 0.8 with mean 5.2 ± 1.3, which suggested the main contribution from biomass burning. Similarly, Thepnuan *et al.* (2019) also described the source emission of PM in Chiang Mai, Thailand, where the annual average OC and EC concentrations, during 2014–2015, were 3.8 ± 2.5 and 1.1 ± 1.1 μg m^{-3} for $PM_{0.1}$ and 2.3 ± 1.6 and 1.4 ± 1.1 μg m^{-3} for $PM_{0.5\text{-}1.0}$ (Phairuang *et al.*, 2019).

Recently, not only black carbon (BC) or EC, but also brown carbon (BrC), which is a fraction of OC, have been identified as light-absorbing carbonaceous aerosols in $PM_{2.5}$ (Pani *et al.*, 2018, 2020, 2021; Tao *et al.*, 2020; Zhang *et al.*, 2021). Radiative forcing (RF) of biomass burning aerosols during dry season in Chiang Mai was –45.3 to –103.4 at the surface and –1.7 to +6.2 W m^{-2} at top of atmosphere corresponding to low - high biomass burning emissions events respectively (Pani *et al.*, 2018). A higher negative RF at the surface indicated a significant decrease in solar radiation, that was enhanced by atmospheric absorption. This agrees with results from a global chemical

transport model (GEOS-Chem) coupled with the rapid radiative transfer model for GCMs (RRTMG) models to study contributions of BC and BrC to light absorption (Zhang *et al.*, 2021). Contributions of BC and BrC were 60–67% and 33–40%, respectively, at 400 nm, consistent with the observation by Pani *et al.* (2021). Instantaneous radiative forcing of carbonaceous $PM_{2.5}$ in Chiang Mai, during the dry season, were about 4–9 times higher than those in rainy seasons. Also, Tao *et al.* (2020) reported that contributions of EC and OC to aerosol absorption coefficients ranged from 49 ± 5 to 79 ± 3% and 21 ± 3 to 51 ± 5%, respectively, in the 370–880 nm region. Hence, the strong light absorption in the ultraviolet and short visible wavelength was closely related with the biomass burning produced carbonaceous aerosols, including BC and BrC. All of these studies were based on $PM_{2.5}$. Thus, it is important to study these effects on finer particles, especially $PM_{0.1}$, because of their recently discovered adverse effects on health as mentioned earlier. However, investigations of $PM_{0.1}$ and its carbonaceous compositions to understand the levels of air pollution, sources, meteorological conditions and impacts in upper SEA, especially during the heavy haze episodes in northern Thailand, are limited and are needed to better understand these phenomena.

We measured $PM_{0.1}$ and carbonaceous aerosols, in particular the EC and OC behaviors, in northern Thailand, during 2017–2019. Atmospheric aerosol samples were collected in Chiang Mai during April 2017, March to April 2018 and March 2019, all during heavy haze periods in Chiang Mai, and compared to the normal period of May 2017 to February 2018. The physical characteristics of $PM_{0.1}$, were studied. OC and EC were analyzed and correlated with the hotspots in the path of the air mass transport by backward trajectories (BT) during the period and the OC/EC ratios were calculated to identify possible sources of $PM_{0.1}$. Influences from meteorological parameters were evaluated.

2 METHODS

2.1 Aerosol Sampling and Physical Characteristics Analysis

Chiang Mai is the largest and one of the most famous cities in the upper SEA: it attracts global tourists, as well as local business persons. It is located in the Chiang Mai-Lamphun basin: the geography consists of high mountains along north-south corridor, covered with forest (69.7%), and agriculture (23.7%) (Land Development Department, 2018). Chiang Mai is typically influenced by transboundary and domestic aerosol transports. Forest fires and agriculture waste burning in northern Thailand are the main sources of haze pollution. Also, aerosol transported from open biomass burning area in some parts of Myanmar and Laos affect the northern Thailand air quality (Thepnuan *et al.*, 2019; Pani *et al.*, 2019). The geography, as well as temperature inversions in the winter, causes air pollution, especially PM, to remain in the region for a prolonged time. Chiang Mai University (CMU), located in the center of Chiang Mai city, Thailand (18°48'09.0''N, 98°57'12.3''E), was selected as a sampling site to confirm the results of physical and chemical characteristics of nanoparticles ($PM_{0.1}$) in the Chiang Mai urban area, as shown in Fig. 1. Samples were taken on the 5th floor of a building, ~16 m above ground to study atmospheric air quality with minimum disturbance from possible local sources (U.S. EPA, 2016). In the present study, we designated the "haze period" as March to April, when significant numbers of hotspots in upper SEA were observed, resulting in high $PM_{2.5}$ concentration in the dry season, as suggested by Pani *et al.* (2019) and Thepnuan *et al.* (2019). The remaining months were labelled the "non-haze period."

Ambient aerosol was sampled using a cascade air sampler capable of segregating particle sizes down to 100 nm, so called $PM_{0.1}$ sampler or nanosampler. The operating air flow was 40 L min^{-1} and sampling time was 24 hr, during the haze periods, and 48 hr, during non-haze periods. Particles were separated into six size ranges: < 0.1 μm ($PM_{0.1}$), 0.1–0.5 μm ($PM_{0.1\text{-}0.5}$), 0.5–1.0 μm ($PM_{0.5\text{-}1}$), 1.0–2.5 μm ($PM_{1\text{-}2.5}$), 2.5–10 μm ($PM_{2.5\text{-}10}$) and > 10 μm ($PM_{>10}$). A 55-mm quartz fiber filter (2500QAT-UP, Pallflex, USA) was used for particle collection in each stage. The stage with an inertial filter (IF) used a stainless-steel filter pack (SUS304, fiber diameter, 9.8 μm) to collect $PM_{0.1\text{-}0.5}$. Before and after collection, the quartz fiber filters were stored in a desiccator with controlled relative humidity 50 ± 5% at room temperature for 72 hrs (Dejchanchaiwong *et al.*, 2020). The filter was then weighed by a 0.01 mg resolution balance (CP225D, Sartorius, Germany).

Five samples during April 2017 and March to April 2018 and seven samples during May 2017–February 2018 were collected to represent 2017–2018 haze and 2017–2018 non-haze periods.

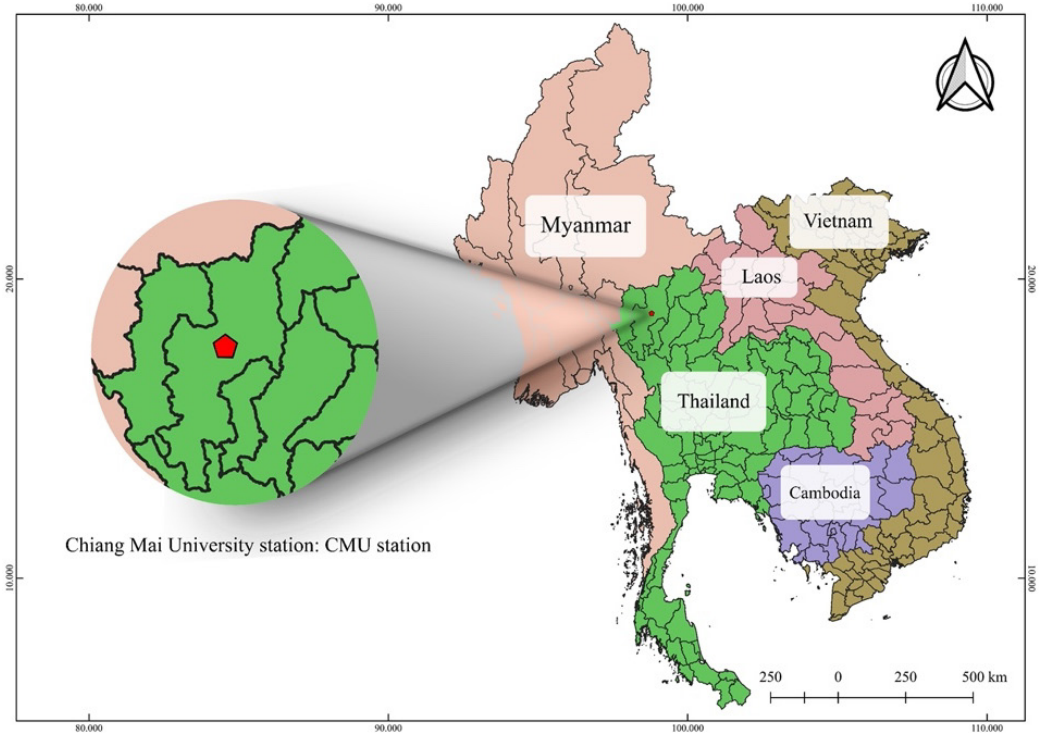

Fig. 1. Sampling locations in Chiang Mai, Thailand.

Seven samples at the same site during the strong haze periods in March 2019 were collected. Sampling details are shown in Table S1. In the following text, 'haze periods' refers to the strong haze periods in years 2017, 2018 and 2019 and 'non-haze periods' refers to the reference, normal periods in years 2017 and 2018.

2.2 Organic and Elemental Carbon Analysis

The carbonaceous components in PM were investigated using a OCEC carbon analyzer (Model 5, Sunset Laboratory, USA), following the Interagency Monitoring of Protected Visual Environments Thermal/Optical Transmittance (IMPROVE_TOT) protocol. OC fractions, including OC1, OC2, OC3 and OC4, were taken at temperatures 120, 250, 450 and 550°C, respectively, in a non-oxidizing helium (He), while the EC fractions, EC1, EC2 and EC3, were taken at 550, 700, 800°C, respectively, in a 2% O_2 and 98% He. The pyrolyzed carbon fraction (PyC) occurred during the transition between EC and OC formation (Chow *et al.*, 2004). Due to a limitation of the carbon aerosol analyzer, samples, collected by the inertial filter, could not be analyzed. Thus, we analyzed only the $PM_{0.1}$ stage to study the nanoparticles in the atmosphere. $PM_{0.1}$ samples, collected uniformly on a backup filter, were punched as 10 × 15 mm^2 rectangles using a cutter. Mass concentration of carbon was calculated from the carbon mass on a punched-out sample, along with the air sampling flow rate, following Phairuang *et al.* (2019).

Quality assurance (QA) and quality control (QC) measures were strictly followed. Field and laboratory blank filters were analyzed. The carbon concentration in the blank filters was subtracted from the samples. Before each carbon analysis, the total carbon (TC) value was calibrated by the reference, sucrose standard (3.206 μg C μL^{-1}) (Sunset Laboratory Inc., USA). The detection limit for the OC/EC carbon analyzer was 0.2 μg C cm^{-2} for both OC and EC analysis. A linear correlation between the sucrose standard solution concentrations and measured concentration was found with R^2 = 0.995. Coefficient of variation of the instrument did not exceed 10% for TC to ensure precision.

The OC was typically derived from primary emission sources and photochemical reactions. Concentrations of primary organic carbon (POC) and secondary organic carbon (SOC) were estimated following the EC-tracer method based on the minimum OC/EC ratio. Since EC and POC are generally emitted from carbon fuel-based combustion processes, which are exclusively associated with primary emissions (Pongpiachan *et al.*, 2014b; Pani *et al.*, 2019), EC is a good

tracer of primary combustion generated OC. The concentrations of POC and SOC were calculated following Eq. (1):

$$POC = EC \times (OC/EC)_{min} \text{ and } SOC = OC - POC \quad (1)$$

2.3 Backward Trajectories and Fire Hotspots-Air Mass Transport Mapping

Aerosol transport from the sources to receptors was simulated to generate 24-hour backward trajectories (BT) at 1,000 m above ground level (AGL) using the Hybrid Single-Particle Lagrangian Integrated Trajectory Model version 4 (HYSPLIT4) (National Oceanic and Atmospheric Administration, 2020). The sampling site (18.79°N, 98.95°E) was chosen to represent the receptor in Chiang Mai. Hotspots from open biomass burning were obtained from the NASA VIIRS 375 m active fire data (Earthdata, 2020). The VIIRS sensor was on the Suomi NPP and NOAA-20 satellites, which are on the same polar orbit, about 50 minutes apart. Each satellite crosses over Thailand twice a day during daylight and the night hours. The observed hotspots could be limited by the orbital times. The present study attempted to evaluate the effects of the fire hotspots on the air quality by assuming the hotspots occurring in the paths of air mass to the receptor influenced PM concentrations. The boundaries of these hotspots were built by connecting each adjacent end point of the air mass trajectories, as shown in Fig. S1. They were calculated by the Geographic Information System (GIS) method to create a shapefile of the area bounding the targeted hotspots. The number of hotspots inside the boundary shapefile was then counted.

3 RESULTS AND DISCUSSION

3.1 $PM_{0.1}$ Mass Concentration

The $PM_{0.1}$ mass concentrations in ambient air at the Chiang Mai (CMU sites) during the haze and non-haze periods are shown in Fig. 2. Concentrations during the haze periods ranged from 6.6 to 19.1 μg m^{-3} with a mean of 12.1 ± 4.0 μg m^{-3}, while during the non-haze periods, they were 3.4 to 6.2 μg m^{-3} with a mean of 4.4 ± 1.0 μg m^{-3}. The values during the haze episode were about 3 times higher than in the non-haze periods. The highest $PM_{0.1}$ concentration, 19.1 μg m^{-3}, occurred during 14–15 March 2019. Contribution of $PM_{0.1}$ was 13.0 ± 3.9% (8.8–20.1%) of the

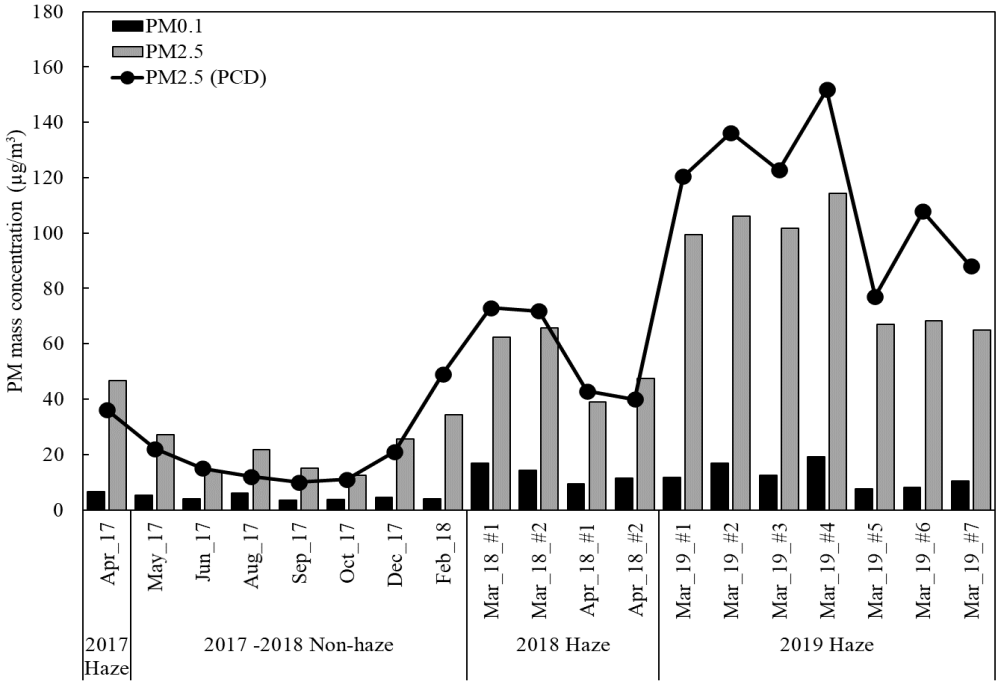

Fig. 2. $PM_{0.1}$ and $PM_{2.5}$ concentrations during the haze (April 2017, March to April 2018 and March 2019) and non-haze periods (May 2017–Febuary 2018).

total suspended particulate (TSP) mass concentrations during the haze periods, and 12.9 ± 2.4% (8.8–15.4%) during the non-haze periods. The $PM_{0.1}$ mass fraction during the haze period in northern Thailand was slightly higher, but the difference was not considered significant. This agrees with measured $PM_{0.1}$ fractions during the haze period in southern Thailand (Chomanee *et al.*, 2020). $PM_{2.5}$ concentrations obtained from the sampling are also shown in Fig. 2. The values were 46.8, 38.9–65.7 and 65.0–114.4 μg m^{-3} during the 2017, 2018 and 2019 haze periods, respectively. They were 12.5–34.4 μg m^{-3} during the 2017 non-haze period. The average contributions of $PM_{0.1}$ in $PM_{2.5}$ were 14.1%, 24.2 ± 2.3% and 13.7 ± 2.4% during the 2017, 2018 and 2019 haze periods, and 22.5 ± 7.0% during the non-haze period. The contributions in the haze periods (2017–2019) were quite different. The change of concentration of submicron particles made a large difference in the $PM_{0.1}/PM_{2.5}$ ratio, because the peak of the particle size distribution, during the haze period, as a result of biomass burning, was usually below 1 micron (Dejchanchaiwong *et al.*, 2020). Ambient $PM_{2.5}$ concentrations were compared to those monitored by the Thailand Pollution Control Department (PCD), located in Mueang District, Chiang Mai Province (18.79°N, 98.98°E), 3.6 km SE of the sampling site. $PM_{2.5}$ concentrations from the sampling were in good agreement with those obtained at the PCD station. The highest $PM_{2.5}$ concentration was 114.4 μg m^{-3} observed on 16–17 March 2019 compared to 151.8 μg m^{-3} at the PCD station. However, the PCD station was in a high traffic city center area, explaining the difference.

3.2 Correlation of PM Concentration with Meteorological Conditions and Fire Hotspots

Meteorological parameters, including precipitation, relative humidity (RH), temperature, wind speed (WS) and wind direction (WD), were obtained from the Thai Meteorological Department, Thailand, as shown in Table S2. Precipitation, during the non-haze period, ranged from 0 to 59.3 mm with mean of 20.1 ± 24.4 mm, and in the haze period from 0–8.5 mm, with mean of 3.1 ± 4.1 mm. Temperatures, during the non-haze and haze periods, were 28.0 ± 2.3°C and 25.3 ± 5.2°C, while RH were 73.5 ± 6.6% and 56.6 ± 7.4%, respectively. Fire hotspots were detected by the VIIRS satellite obtained from Fire Information for Resource Management System (Earthdata, 2020) and counted by the GIS method described in Sec 1.3.

Linear correlations between $PM_{0.1}$ concentration and meteorological parameters and number of fire hotspots are shown in Table 1. The best correlations for the entire period were $PM_{0.1}$ with relative humidity and number of hotspots (R^2 = 0.68 and 0.53, respectively). The positive slope of $PM_{0.1}$ versus number of hotspots indicated a strong influence from the biomass burning, which occurred in the dry season, as suggested by the negative correlation between $PM_{0.1}$ and RH correlation. On the other hand, correlations between $PM_{0.1}$ mass concentrations and precipitation, temperature and wind speed were not strong. High wind speeds and precipitation favored the dispersion of atmospheric pollutants and reduced PM concentrations, while low wind speeds and low precipitation helped pollution levels to rise. Typically, temperature inversion plays an important role in high accumulation of air pollution during the winter months. In Chiang Mai, it usually occurs from November to March (Wiriya *et al.*, 2013). During the 2018 haze periods, temperature inversion, from ground to 606 m, was observed only on 21 March. In 2019, it occurred from ground to 476–658 AGL during 12–25 March. Atmospheric temperature data was taken from the Department of Atmospheric Science, University of Wyoming, radiosonde database (University of Wyoming, 2021). This caused low levels of planetary boundary layer (PBL) and the aerosols, including $PM_{0.1}$, to be trapped and difficult to ventilate.

Table 1. Correlation coefficients: $PM_{0.1}$ concentration *vs* meteorological parameters.

Parameters	Linear regression model	
	Slope	R^2
Precipitation	–1.91	0.14
Temperature	0.21	0.17
Relative humidity	–2.14	0.68
Wind speed	–0.12	0.11
Number of hotspots	0.003	0.53

Table 2. Average OC and EC concentrations and OC/EC ratios in $PM_{0.1}$ particles during haze and non-haze periods in Chiang Mai.

Period	Concentration (μg m^{-3})						
	$PM_{0.1}$	OC	EC	TC	POC	SOC	
Haze	12.1 ± 4.0	6.8 ± 2.7	1.4 ± 0.5	8.2 ± 3.2	5.2 ± 2.0	1.6 ± 1.2	
Non-haze	4.4 ± 1.0	1.9 ± 0.9	0.5 ± 0.2	2.4 ± 1.1	1.6 ± 0.8	0.3 ± 0.3	
Period	Ratio (-)						
	TC/PM	OC/PM	EC/PM	OC/TC	EC/TC	OC/EC	ECR
Haze	0.7 ± 0.2	0.6 ± 0.1	0.1 ± 0.03	0.8 ± 0.1	0.2 ± 0.1	5.0 ± 1.0	0.3 ± 0.2
Non-haze	0.5 ± 0.3	0.4 ± 0.2	0.1 ± 0.1	0.8 ± 0.02	0.2 ± 0.02	3.7 ± 0.5	0.1 ± 0.1

3.3 OC and EC Characteristics during Haze and Non-haze Periods in $PM_{0.1}$ Particles

The average OC, EC, total carbon (TC), POC and SOC concentrations, TC/PM, EC/TC, OC/EC and effective carbon ratio (ECR) ratios (defined in Sec. 3.4) for $PM_{0.1}$ during the haze and non-haze periods in Chiang Mai are listed in Table 2. Average TC mass concentrations in $PM_{0.1}$ were 8.2 ± 3.2 μg m^{-3} during the haze periods, approximately 4 times higher than the value of 2.4 ± 1.1 μg m^{-3} during the non-haze periods. The high TC/PM portion was found in $PM_{0.1}$ during both the haze (0.7 ± 0.2) and non-haze (0.5 ± 0.3) periods. This agrees with previous studies by Phairuang *et al.* (2019) and Dejchanchaiwong *et al.* (2020), indicating that $PM_{0.1}$ particles were the significant carcinogenic emission during both periods. The average OC concentration in $PM_{0.1}$ during the haze periods was 6.8 ± 2.7 μg m^{-3}, nearly 4 times higher than that during the non-haze periods, where average OC concentration was 1.9 ± 0.9 μg m^{-3}. Average EC concentrations in $PM_{0.1}$ during the haze periods were 1.4 ± 0.5 μg m^{-3}, approximately 3 times higher than the non-haze periods. During haze periods, contributions to $PM_{0.1}$ mass concentration were OC (57.1 ± 14.2%) and EC (11.7 ± 3.3%), whereas during the non-haze periods, they were 40.7 ± 24.4% and 11.0 ± 6.3%, respectively. It is significant to note that carbonaceous aerosols were a large component of $PM_{0.1}$, accounting for 51.8 ± 30.57%–68.7 ± 16.9% of $PM_{0.1}$ mass.

3.4 Primary and Secondary Organic Carbon in $PM_{0.1}$

The fractional contributions of POC and SOC in total OC during the haze and non-haze periods are shown Fig. S2. The average POC and SOC concentrations in $PM_{0.1}$, during the haze period, were 5.2 ± 2.0 μg m^{-3} (78.4 ± 13.9% in OC), and 1.6 ± 1.2 μg m^{-3} (21.6 ± 13.9% in OC) respectively. On the other hand, the average POC and SOC during the non-haze periods were 1.6 ± 0.8 μg m^{-3} (87.1 ± 12.7% in OC) and 0.3 ± 0.3 μg m^{-3} (12.9 ± 12.7% in OC), respectively. The fractional contribution of SOC to total OC increased during the haze periods, compared to the non-haze periods, because the increasing PM concentration provided more organic precursors to react with the volatile organic compounds (VOCs) and scattered the solar radiation, leading to increasing SOC formation (Ramirez *et al.*, 2018, Pani *et al.*, 2019). However, this increase in SOC was not sufficient to overcome the dominance of POC, which confirmed the primary source of aerosol during both periods in the region, because POC is linked to primary emissions (Pani *et al.*, 2019). This also agrees with results of OC and EC analysis from $PM_{2.5}$ in Poland (Błaszczak *et al.*, 2020).

3.5 Effective Carbon Ratio (ECR)

The POC and SOC are produced with different mechanisms, i.e., different interactions with solar radiation (Ramirez *et al.*, 2018). The POC and EC or black carbon (BC) commonly originate from the same emission sources, i.e., biomass burning, cooking and vehicles exhaust, and generally absorb solar radiation, whereas SOC mainly originates from photochemical reaction and scatters it (Safai *et al.*, 2014). However, BrC, which is a fraction of OC, has recently been found to strongly absorb light in the ultraviolet and short visible wavelength regions (Pani *et al.*, 2018; Pani *et al.*, 2020; Pani *et al.*, 2021). The effective carbon ratio (ECR) was estimated to understand the relation between carbonaceous aerosols and climate impact (Safai *et al.*, 2014; Ramirez *et al.*, 2018):

$$ECR = SOC/(POC + EC) \quad (2)$$

In the present study, the average ECRs in $PM_{0.1}$ were 0.3 ± 0.2 during the haze and 0.1 ± 0.1 during the non-haze periods, as shown in Table 2. A higher ECR value during the haze period was observed due to a higher SOC concentration. SOC was previously believed to be light scattering carbonaceous aerosol (Safai *et al.*, 2014; Singh *et al.*, 2016; Ramirez *et al.*, 2018). The presence of BrC in SOC could reduce the strong light scattering characteristics. However, an increase of ECR as a result of higher SOC along with high $PM_{0.1}$ concentration during the haze period should lead to higher potential for global warming. However, lower ECRs due to the lower SOC concentrations during the non-haze period did not indicate significant atmospheric warming because of low PM concentration.

3.6 OC/EC Ratios of $PM_{0.1}$ Particles

The average OC/EC ratios in the present and previous studies in Thailand are shown in Table 3. Most studies used thermal optical reflectance (TOR). OC/EC ratios results, using IMPROVE_TOT methods in this study, were corrected to OC/EC ratios, based on the IMPROVE_TOR equation of Han *et al.* (2016), who compared OC and EC measurements in Xi'an, China, and are also shown in Table 3. Ratios of IMPROVE_TOT to IMPROVE_TOR were 1.22 for OC concentration (R^2 = 0.99) and 0.6 for EC concentration (R^2 = 0.95). Hence, discrepancies between TOR and TOT for OC and EC were smaller, when measured by the IMPROVE protocol. EC measured, using the TOT method, was lower than the TOR method. This is because PyC calculated by TOT was delayed and split the OC and EC more than values derived from reflectance measurements (Chow *et al.*, 2004; Han *et al.*, 2009; Han *et al.*, 2016). In addition, Han *et al.* (2016) reported that OC/EC ratios in $PM_{2.5}$ of ambient air, by IMPROVE_TOT (OC/EC: 2.3–6.7), were approximately 2 times higher than those using IMPROVE_TOR (OC/EC: 1.4–3.7), while average OC/EC ratios for biomass combustion emission by IMPROVE_TOT (OC/EC: 4.6–19.3) were higher than those by IMPROVE_TOR (OC/EC 3.1–10.8). This agrees with Khan *et al.* (2012), who reported that the average OC/EC ratios for IMPROVE_TOT were higher than with IMPROVE_TOR, with average TOT/TOR ratio of 1.2 for diesel and 1.4 for cooking stove combustion emission.

In the present study, average OC/EC ratios in $PM_{0.1}$, based on the IMPROVE_TOT method, during haze periods, ranged from 3.6-6.8, with mean of 5.0 ± 1.0 and ranged from 3.0–4.2 (mean 3.7 ± 0.5), during non-haze periods. Results showed that the corrected OC/EC ratios in $PM_{0.1}$, based on IMPROVE_TOR, during the haze periods, ranged from 1.8-3.3 (mean 2.5 ± 0.5,) versus from 1.5–2.1 (mean 1.8 ± 0.3), during the non-haze periods. Phairuang *et al.* (2019) also reported $PM_{0.1}$ OC/EC ratios, in Chiang Mai, were about 3.4 and suggested the main contribution was from biomass burning. Khan *et al.* (2012) reported that the average OC/EC ratios based on the IMPROVE_TOT method in $PM_{2.5}$ were 0.1–0.97 for diesel exhaust. Additionally, Zhu *et al.* (2010) reported $PM_{0.1}$ OC/EC ratios, based on IMPROVE_TOR, were 0.68, due to motor vehicle fuel combustion. It can be seen that both the OC/EC ratios, exceeding 1.0, based on IMPROVE_TOT and IMPROVE_TOR methods, can be attributed to the biomass burning emission. Hence, the high values of OC/EC based on IMPROVE_TOT and IMPROVE_TOR methods in $PM_{0.1}$ during haze periods in the present study can be explained by increasing contribution from biomass burning emissions. This is in agreement with the studies of PM emission sources in Chiang Mai, Thailand (Pongpiachan *et al.*, 2013; Pani *et al.*, 2019). The vehicular emissions dominated EC during the non-haze period because of the generally high concentration of traffic in Chiang Mai city. This was confirmed by the low OC/EC ratios.

3.7 Distributions of Carbonaceous Components in $PM_{0.1}$

Eight carbon fractions are often used for source identification of the carbonaceous aerosols. OC3 and EC1-PyC are the most abundant fractions of OC in biomass burning (Cao *et al.*, 2005; Chuang *et al.*, 2013; Pani *et al.*, 2019). OC2 represents the secondary organic carbon (SOC) formation, as well as coal combustion and biomass burning, and is also the major fraction of OC in motor vehicle exhaust (Chow *et al.*, 2004). Moreover, PyC represents incomplete combustion during cooking and biomass burning (Cao *et al.*, 2005). EC2 and EC3 are good indicators of hot-gas evaporation from motor vehicles (Phairuang *et al.*, 2019). Eight carbonaceous fractions and concentrations in $PM_{0.1}$ during the haze and non-haze periods from this study are shown in Fig. S3. During the haze periods, the order of OC and EC fraction in $PM_{0.1}$ was PyC > OC3 > OC2 > OC4 > EC2 > (EC1 – PyC)

ORIGINAL RESEARCH
https://doi.org/10.4209/aaqr.210069

Table 3. OC and EC concentrations and OC/EC ratios- present and previous Thai studies.

Sites	Periods	Methods	Particle size	PM ($\mu g\ m^{-3}$)	OC ($\mu g\ m^{-3}$)	EC ($\mu g\ m^{-3}$)	OC/EC	References
Chiang Mai	Haze, April 2017 March–April 2018 April 2019	IMPROVE_TOT	$PM_{0.1}$	12.1 ± 4.0	6.8 ± 2.7	1.4 ± 0.5	5.0 ± 1.0	Present study
	Non-haze, May 2017–February 2018		$PM_{0.1}$	4.4 ± 1.0	1.9 ± 0.9	0.5 ± 0.2	3.7 ± 0.5	
	Haze	IMPROVE_TOR	$PM_{0.1}$	12.1 ± 4.0	5.6 ± 2.2	2.3 ± 0.9	2.5 ± 0.5	
	Non-haze	(corrected by equation of Han *et al.*, 2016)	$PM_{0.1}$	4.4 ± 1.0	1.5 ± 0.8	0.8 ± 0.4	1.8 ± 0.3	
	Dry season, March 2015	IMPROVE_TOR	$PM_{0.1}$	25.2 ± 4.7	3.8 ± 2.5	1.1 ± 1.1	3.5	Phairuang *et al.* (2019)
	Dry season, February–April 2016	IMPROVE_TOR	$PM_{2.5}$	64.3 ± 17.6	23.6 ± 8.1	2.8 ± 1.0	3.6–11.0	Thepnuan *et al.* (2019)
	Haze, March 2015	IMPROVE_TOR	$PM_{2.5}$	113 ± 45	46.6 ± 19.0	9.5 ± 4.3	5.2 ± 1.3	Pani *et al.* (2019)
	February 2008	IMPROVE_TOR	PM_{10}	92.3 ± 28.1	30.8 ± 13.6	5.3 ± 2.6	5.8 ± 3.9	Pongpiachan *et al.* (2013)
Bangkok	Haze, December 2018–January 2019	IMPROVE_TOR	$PM_{0.1}$	11.4 ± 4.7	2.2 ± 0.3	0.8 ± 0.1	3.0 ± 0.6	Dejchanchaiwong *et al.* (2020)
	February–December, 2007	IMPROVE_TOR	PM_{10}	–	10.0 ± 2.7	10.1 ± 4.3	1.0 ± 0.6	Pongpiachan *et al.* (2014)
Songkhla	January–December 2018	IMPROVE_TOR	$PM_{0.1}$	10.2 ± 2.2	0.7 ± 0.6	0.2 ± 0.1	2.9	Phairuang *et al.* (2020)
Xi'an, Chia	March 10, 2012–March 11, 2013	IMPROVE_TOT	$PM_{2.5}$	–	21.2+11.5	5.6 ± 3.3	4.1 ± 1.0	Han *et al.* (2016)
		IMPROVE_TOR	$PM_{2.5}$	–	17.5 ± 9.1	9.3 ± 5.7	2.04 ± 0.5	

> EC3 > OC1, while, during the non-haze periods, it was OC2 > OC3 > OC4 > PyC > EC2 > EC3 > (EC1 – PyC) > OC1.

OC3 and OC2 were the most abundant fractions of OC in $PM_{0.1}$, during both haze and non-haze periods, indicating the significant contribution of biomass burning to carbonaceous aerosols. The OC1 fraction in $PM_{0.1}$ mostly contains volatile organic substances, which can rapidly evaporate during long-range transport (Lee *et al.*, 2016). Our results agree with a previous study of OC and EC distributions to $PM_{0.1}$ (Phairuang *et al.*, 2019)

3.8 Correlations between OC and EC, and OC/EC and Number of Hotpots

Correlation analysis is usually used to determine whether the pollution sources of OC and EC are consistent (Han *et al.*, 2009; Zhang *et al.*, 2011; He *et al.*, 2015; Guo, 2016; Wang *et al.*, 2017). Correlations between OC and EC in $PM_{0.1}$, during the haze and non-haze periods, are shown in Fig. 3. Strong OC and EC correlations during the non-haze periods (R^2 = 0.91) suggested impacts from a combination of common and consistent sources, particularly motor vehicle exhaust and biomass burning, which was dominant in the area (Cao *et al.*, 2007). However, the correlation was lower during the haze periods (R^2 = 0.80), implying a more complex pattern of emission sources (Cao *et al.*, 2007). The OC vs. EC slope during the haze periods (2.28) was higher than during the non-haze periods (1.84). This indicated a larger contribution of OC in the carbonaceous aerosol from primary emissions of various biomass burnings during the haze periods: the major emission source at those times in the north of Thailand is fire in deciduous forests. The other major source was agricultural waste (Wiriya *et al.*, 2013, 2016; Thepnuan *et al.*, 2019; Pani *et al.*, 2019). The intercepts between OC & EC relations were very small and acceptably close to the ideal zeroes, when no sources were present.

Influence from biomass burning can be confirmed by the number of fire hotspots in the path of the wind to the receptor. During the haze periods, OC/EC ratio increased linearly with hotspot numbers and at nearly twice the slope in the non-haze periods, see Fig. 4. The positive correlation was stronger for the haze periods (R^2 = 0.42) than the non-haze period (R^2 = 0.26). This suggested larger contributions from biomass burning when the hotspots were increased. The intercepts from both correlations, 1.77 and 1.97, were very close and confirmed the good agreement, when no hotspots were present. The low OC/EC ratios indicated the $PM_{0.1}$ from other sources, particularly emission from diesel engines, because Chiang Mai is a congested city with significant traffic problems (Pongpiachan *et al.*, 2014a; Phairuang *et al.*, 2019; Thepnuan *et al.*, 2019). The hotspots-air mass transport mapping technique used here allowed an appropriate evaluation of the biomass burning source contribution to the $PM_{0.1}$ concentration at the receptor.

3.9 Backward Trajectories

Backward trajectory simulations for Chiang Mai during the haze and the non-haze periods are shown in Fig. S4. High $PM_{0.1}$ concentrations during the haze periods were correlated with a trajectory

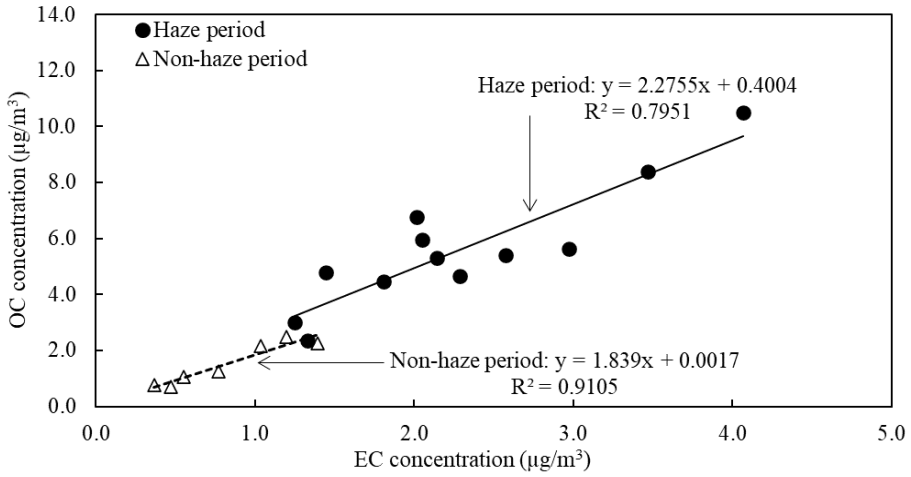

Fig. 3. Correlation OC vs. EC in $PM_{0.1}$ during non-haze and haze periods.

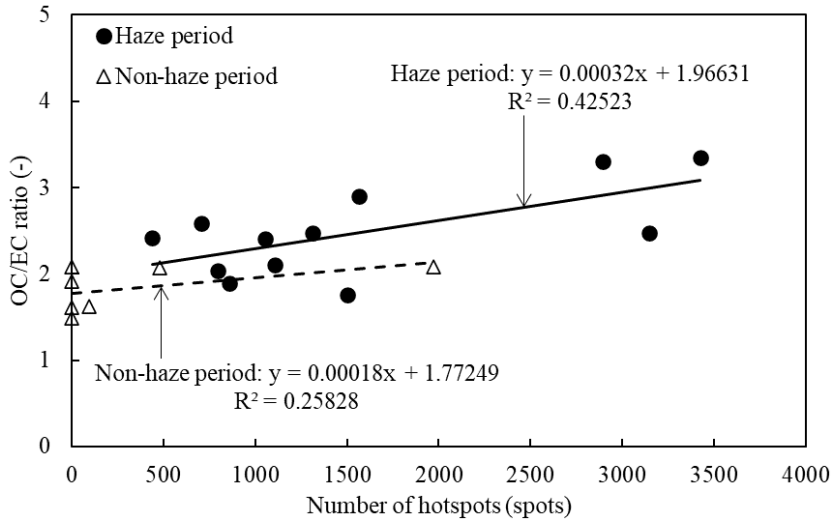

Fig. 4. Correlation between OC/EC ration in $PM_{0.1}$ and number of hotspots during non-haze and haze periods.

from south to north and west to east. Wind simulation on April 3, 2017 (Fig. S4(a)) showed that the east and west wind moved towards Chiang Mai mostly from northern Thailand and also some parts of Laos and Myanmar, where partial hotspots were observed. Backward trajectories, on March 2018 and 2019, showed west and southwest bound air masses, passing through some hotspots in Myanmar, to Chiang Mai (Figs. S4(b) and S4(d)). Also, south wind flowed to Chiang Mai from the west and northern Thailand, where high numbers of biomass burning hotspots, from agriculture residues, were observed, along with some parts of Myanmar (Fig. S4(c)). Open biomass burning in the forest has been a major local source affecting air quality in northern Thailand. It contributed 90% of about 1 Mha of burnt area during the 2019 dry season, whereas the remainder was from agricultural waste burning (GISDA, 2020). Simulation during the non-haze periods, on the other hand, showed that the air mass moved from southwest to Chiang Mai in August 2017 carrying clean air from Indian Ocean and no hotspots occurred during this period (Fig. S4(e)). Wind trajectories in October 2017 clearly confirmed that that there was no significant domestic and transboundary haze transport (Fig. S4(f)). Hence, the 48-hrs backward trajectories during the haze periods showed aerosol transported from open biomass burning areas, in Thailand and some parts of Myanmar, affected the Chiang Mai air quality, especially its PM concentrations due to east to west winds. This confirms previous studies of potential PM sources in Chiang Mai (Wiriya *et al.*, 2013; Wiriya *et al.*, 2016; Thepnuan *et al.*, 2019; Pani *et al.*, 2019; Phairuang *et al.*, 2019).

4 CONCLUSIONS

Physical characteristics and carbonaceous components in $PM_{0.1}$, during the haze and non-haze periods in Chiang Mai, Thailand were investigated to identify and characterize sources of haze pollution. We conclude:

- The $PM_{0.1}$ level during the haze periods was significantly higher: the average $PM_{0.1}$ concentration during the haze periods (12.1 ± 4.0 μg m^{-3}) was about 3 times as high as the non-haze periods (4.4 ± 1.0 μg m^{-3}). $PM_{0.1}$ concentration was strongly negatively correlated with relative humidity and positively correlated with hotspot numbers.
- OC concentrations during the haze and non-haze periods were 6.8 ± 2.7 μg m^{-3} and 1.9 ± 0.9 μg m^{-3}, whereas EC concentrations were 1.4 ± 0.5 and 0.5 ± 0.2 μg m^{-3}, respectively, i.e., OC and EC concentrations were about 3 and 4 times higher during the haze periods. The OC fraction in $PM_{0.1}$ was also affected by long-range transport and secondary organic aerosol formation, because the contribution of SOC to total OC during the haze periods also increased relative to the non-haze periods.
- Strong OC and EC correlation ($R^2 = 0.91$), during non-haze periods, indicated a combination

of common and consistent sources, whereas the lower correlation (R^2 = 0.80) during haze period suggested a more complex pattern of emission source. The OC/EC ratio and number of hotspots correlation was stronger for the haze periods (R^2 = 0.42) than the non-haze period (R^2 = 0.26).

- The high $PM_{0.1}$ concentration and OC/EC ratio indicated more contribution from various biomass burning to the $PM_{0.1}$ during the haze periods. The 48-hr backward trajectories confirmed this. An increase of OC and EC, the light-absorbing carbonaceous aerosols, may also significantly impact regional air quality and climate in Chiang Mai and upper SEA.

This study enhanced knowledge of carbonaceous aerosol in $PM_{0.1}$ over upper SEA and emission control strategies on $PM_{0.1}$ of ambient air. This should be of concern because $PM_{0.1}$ has adverse effects on humans and the atmospheric environment.

ACKNOWLEDGMENTS

This research was financially supported by the Biodiversity-based Economy Development Office (BEDO) of Thailand under grant number ENG590707S. This work was also supported by the Interdisciplinary Graduate School of Energy Systems, Prince of Songkla University under grant number 1-2018/08. We would like to thank Chevron Thailand Exploration and Production, Ltd. for manufacturing a nice and sharp filter cutter. Additionally, we would like to thank the Faculty of Environment, Kasetsart University for providing the OCEC carbon analyzer. We acknowledge Dr. Worradorn Phairuang for his carbon analysis consultation, and are also thankful to John Morris for English language editing.

SUPPLEMENTARY MATERIAL

Supplementary material for this article can be found in the online version at https://doi.org/10.4209/aaqr.210069

REFERENCES

Apte, J.S., Brauer, M., Cohen, A.J., Ezzati, M., Pop III, C.A. (2018). Ambient $PM_{2.5}$ reduces global and regional life expectancy. Environ. Sci. Technol. Lett. 5, 546–551. https://doi.org/10.1021/acs.estlett.8b00360

ASEAN Specialized Meteorological Centre (ASMC) (2020). http://asmc.asean.org/home/ (accessed 31 July 2020).

Cao, J.J., Wu, F., Chow, J.C., Lee, S.C., Li, Y., Chen, S.W., An, Z.S., Fung, K.K., Watson, J.G., Zhu, C.S., Liu, S.X. (2005). Characterization and source apportionment of atmospheric organic and elemental carbon during fall and winter of 2003 in Xi'an, China. Atmos. Chem. Phys. 5, 3127–3137. https://doi.org/10.5194/acp-5-3127-2005

Cao, J.J., Lee, S.C., Chow, J.C., Watson, J.G., Ho, K.F., Zhang, R.J., Jin, Z.D., Shen, Z.X., Chen, G.C., Kang, Y.M., Zou, S.C., Zhang, L.Z., Qi, S.H., Dai, M.H., Cheng, Y., Hu, K. (2007). Spatial and seasonal distributions of carbonaceous aerosols over China. J. Geophys. Res. 112, D22S11. https://doi.org/10.1029/2006JD008205

Cheng, H., Saffari, A., Sioutas, C., Forman, H.J., Morgan, T.E., Finch, C.E. (2016). Nanoscale particulate matter from urban traffic rapidly induces oxidative stress and inflammation in olfactory epithelium with concomitant effects on brain. Environ Health Perspect. 124, 1537–1546. https://doi.org/10.1289/EHP134

Chomanee, J., Thongboon, K., Tekasakul, S., Furuuchi, M., Dejchanchaiwong, R., Tekasakul, P. (2020). Physicochemical and toxicological characteristics of nanoparticles in aerosols in southern Thailand during recent haze episodes in lower Southeast Asia. J. Environ. Sci. 94, 72–80. https://doi.org/10.1016/j.jes.2020.03.021

ChooChuay, C., Pongpiachan, S., Tipmanee, D., Deelaman, W., Iadtem, N., Suttinun, O., Wang, Q., Xing, L., Li, G., Han, Y., Hashmi, M.Z. Palakun, J., Poshyachinda, S., Aukkaravittayapun, S., Surapipith, V., Cao, J. (2020a). Effects of agricultural waste burning on $PM_{2.5}$-bound polycyclic

aromatic hydrocarbons, carbonaceous compositions, and water-soluble ionic species in the ambient air of Chiang-Mai, Thailand. Polycyclic Aromat. Compd. https://doi.org/10.1080/10406638.2020.1750436

ChooChuay, C., Pongpiachan, S., Tipmanee, D., Deelaman, W., Suttinun, O., Wang, Q., Xing, L, Li, G., Han, Y., Palakun, J., Poshyachinda, S., Aukkaravittayapun, S., Surapipith, V., Cao, J. (2020b). Long-range transboundary atmospheric transport of polycyclic aromatic hydrocarbons, carbonaceous compositions, and water-soluble ionic species in southern Thailand. Aerosol Air Qual. Res. 20, 1591–1606. https://doi.org/10.4209/aaqr.2020.03.0120

ChooChuay, C., Pongpiachan, S., Tipmanee, D., N., Suttinun, O., Deelaman, W., Wang, Q., Xing, L., Li, G., Han, Y., Palakun, J., Cao, J. (2020c). Impacts of $PM_{2.5}$ sources on variations in particulate chemical compounds in ambient air of Bangkok, Thailand. Atmos. Pollut. Res. 11, 1657–1667. https://doi.org/10.1016/j.apr.2020.06.030

Chow, J.C., Watson, J.G., Chen, L.W.A., Arnott, W.P., Moosmuller, H. (2004). Equivalence of elemental carbon by thermal/optical reflectance and transmittance with different temperature protocols. Environ. Sci. Technol. 38, 4414–4422. https://doi.org/10.1021/es034936u

Chow, J.C., Watson, J.G., Louie, P.K.K., Chen, L.W.A., Sin, D. (2005). Comparison of $PM_{2.5}$ carbon measurement methods in Hong Kong, China. Environ. Pollut. 137, 334–344. http://doi.10.1016/j.envpol.2005.01.006

Chow, J.C., Watson, J.G., Chen, L.W.A., Chang, M.C.O., Robinson, N.F., Trimble, D., Kohl, S. (2007). The IMPROVE-A temperature protocol for thermal/optical carbon analysis: Maintaining consistency with a long-term database. J. Air Waste Manage. Assoc. 57, 1014–1023. https://doi.org/10.3155/1047-3289.57.9.1014

Chu, S.H. (2005). Stable estimate of primary OC/EC ratios in the EC tracer method. Atmos. Environ. 39, 1383–1392. https://doi.org/10.1016/j.atmosenv.2004.11.038

Chuang, H.C., Hsiao, T.C., Wang, S.H., Tsai, S.C., Lin, N.H. (2016). Characteristic of particulate matter profiling and aevolar deposition from biomass burning in Northern Thailand: The 7-SEAS study. Aerosol Air Qual. Res. 16, 2897–2906. https://doi.org/10.4209/aaqr.2015.08.0502

Chuang, M.T., Chou, C.K., Sopajareepom, K., Lin, N.H., Wang, J.L., Sheu, G.R., Chang, Y.J., Lee, C. (2013). Characterization of aerosol chemical properties from near-source biomass burning in Chiang Mai, Thailand during 7-SEAS/Dongsha experiment. Atmos. Environ. 78, 72–81. https://doi.org/10.1016/j.atmosenv.2012.06.056

Dejchanchaiwong, R., Tekasakul, P. Tekasakul, S., Phairuang, W., Nim, N., Thongboon, K., Rhongyen, T., Suwattiga, P. (2020). Impact of transport of fine and ultrafine particles from biomass open burning on air quality during 2019 Bangkok haze episode. J. Environ. Sci. 97, 149–161. https://doi.org/10.1016/j.jes.2020.04.009

Dejchanchaiwong, R., Tekasakul, P. (2021). Effects of coronavirus induced city lockdown on $PM_{2.5}$ and gaseous pollutant concentrations in Bangkok. Aerosol Air Qual. Res. 21, 200418. https://doi.org/10.4209/aaqr.200418

Earthdata (2020). NRT VIIRS 375 m Active Fire product VNP14IMGT. https://earthdata.nasa.gov/firms (accessed 15 July 2020).

GISTDA (2020). Thailand fire monitor. http://fire.gistda.or.th/ (accessed 15 July 2020).

Hahad, O., Lelieveld, J., Birklein, F., Lieb, K., Daiber, A., Münzel, T. (2020). Ambient air pollution increases the risk of cerebrovascular and neuropsychiatric disorders through induction of inflammation and oxidative stress. Int. J. Mol. Sci. 21, 4306. https://doi.org/10.3390/ijms21124306

Han, Y.M., Cao, J.J., Chow, J.C., Watson, J.G., An, Z.S., Liu, S.X. (2009). Elemental carbon in urban soils and road dusts in Xi'an, China and its implication for air pollution. Atmos. Environ. 43, 2464–2470. https://doi.org/10.1016/j.atmosenv.2009.01.040

Han, Y.M., Chen, L.W.A., Huang, R.J., Chow, J.C., Watson, J.G., Ni, H.Y., Liu, S.X., Fung, K.K., Shen, Z.X., Wang, Q.Y., Tian, J., Zhao, Z.Z., Prevot A.S.H., Cao, J.J. (2016). Carbonaceous aerosols in megacity Xi'an, China: Implications of thermal/optical protocols comparison. Atmos. Environ. 132, 58–68. https://doi.org/10.1016/j.atmosenv.2016.02.023

Haque, Md. M., Kawamura, K., Deshmukh, D.K., Fang, C., Song, W., Mengying, B., Zhang, Y.L. (2019). Characterization of organic aerosols from a Chinese megacity during winter: Predominance of fossil fuel combustion. Atmos. Chem. Phys. 19, 5147–5164, https://doi.org/10.5194/acp-19-5147-2019

Hata, M., Chomanee, J., Thongyen, T., Bao, L., Tekasakul, S., Tekasakul, P., Otani, Y., Furuuchi, M. (2014). Characteristics of nanoparticles emitted from burning of biomass fuels. J. Environ. Sci. 26, 1913–1920. https://doi.org/10.1016/j.jes.2014.07.005

Huang, R.J., Zhang, Y., Bozzetti, C., Ho, K.F., Cao, J.J., Han, Y., Daellenbach, K.R., Slowik, J.G., Platt, S.M., Canonaco, F., Zotter, P., Wolf, R., Pieber, S.M., Bruns, E.A., Crippa, M., Ciarelli, G., Piazzalunga, A., Schwikowski, M., Abbaszade, G., Schnelle-Kreis, J., *et al.* (2014). High secondary aerosol contribution to particulate pollution during haze events in China. Nature 514, 218–222. https://doi.org/10.1038/nature13774

Jew, K., Herr, D., Wong, C.Kennell, A., Schaffer, M.K.., Oberdorster, G., O'Banion, M.K., Cory-Slechta, D.A., Elder, A. (2019). Selective memory and behavioral alterations after ambient ultrafine particulate matter exposure in aged 3xTgAD Alzheimer's disease mice. Part. Fibre. Toxicol. 16, 45. https://doi.org/10.1186/s12989-019-0323-3

Khan, B., Hays, M.D., Geron, C., Jetter, J. (2012). Differences in the OC/EC ratios that characterize ambient and source aerosols due to thermal-optical analysis. Aerosol Sci. Technol. 46, 127–137. https://doi.org/10.1080/02786826.2011.609194

Le, H.A. (2020). Emission inventories of rice straw open burning in the Red River Delta of Vietnam: Evaluation of the potential of satellite data. Environ. Pollut. 260, 113972. https://doi.org/10.1016/j.envpol.2020.113972

Lee, C.T., Ram, S.S., Nguyen, D.L., Chou, C.C., Chang, S.Y., Lin, N.H., Chang, S.C., Hsiao, T.C., Sheu, G.R., Ou-Yang, C.F., Chi, K.H., Wang, S.H., Wu, X.C. (2016). Aerosol chemical profile of near-source biomass burning smoke in Sonla, Vietnam during 7-SEAS campaigns in 2012 and 2013. Aerosol Air Qual. Res. 16, 2603–2617. https://doi.org/10.4209/aaqr.2015.07.0465

Li, W., Shao, L. (2009). Transmission electron microscopy study of aerosol particles from the brown hazes in northern China. J. Geophys. Res. 114, D09302. https://doi.org/10.1029/2008JD011285

Li, W., Shao, L., Zhang, D., Ro, C.U., Hu, M., Bi, X., Geng, H., Matsuki, A., Niu, H., Chen, J. (2016). A review of single aerosol particle studies in the atmosphere of East Asia: Morphology, mixing state, source, and heterogeneous reactions. J. Cleaner Prod. 112, 1330–1349. https://doi.org/10.1016/j.jclepro.2015.04.050

Morris-Schaffer, K., Merrill, A., Jew, K., Wong, C., Conrad, K., Harvey, K., Marvin, E., Sobolewski, M., Oberdörster, G., Elder, A., Cory-Slechta, D.A. (2019). Effects of neonatal inhalation exposure to ultrafine carbon particles on pathology and behavioral outcomes in C57BL/6J mice. Part. Fibre. Toxicol. 16, 10. https://doi.org/10.1186/s12989-019-0293-5

National Oceanic and Atmospheric Administration (NASA) (2020). HYSPLIT Trajectory Model. Air Resources Laboratory, NOAA's Office of Atmospheric Research, NASA. https://www.ready.noaa.gov/hypub-bin/trajtype.pl?runtype=archive (accessed 31 July 2020).

Nguyen, G.T.H., Shimadera, H., Uranishi, K., Matsuo, T., Kondo, A. (2019). Numerical assessment of $PM_{2.5}$ and O_3 air quality in Continental Southeast Asia: Impacts of potential future climate change. Atmos. Environ. 215, 116901. https://doi.org/10.1016/j.atmosenv.2019.116901

Pani, S.K., Lin, N.H., Chantara, S., Wang, S.H., Khamkaew, C., Prapamontol, T., Janjai, S. (2018). Radiative response of biomass-burning aerosols over an urban atmosphere in northern peninsular Southeast Asia. Sci. Total Environ. 633, 892–911. https://doi.org/10.1016/j.scitotenv.2018.03.204

Pani, S.K., Chantara, S., Khamkaew, C., Lee, C., Lin, N.H. (2019). Biomass burning in the northern peninsular Southeast Asia: Aerosol chemical profile and potential exposure. Atmos. Res. 224, 180–195. https://doi.org/10.1016/j.atmosres.2019.03.031

Pani, S.K., Wang, S.H., Lin, N.H., Chantara, S., Lee, C.T., Thepnuan, D. (2020). Black carbon over an urban atmosphere in northern peninsular Southeast Asia: Characteristics, source apportionment, and associated health risks. Environ. Pollut. 259, 113871. https://doi.org/10.1016/j.envpol.2019.113871

Pani, S.K., Lin, N.H., Griffith, S.M., Chantara, S., Lee, C.T., Thepnuan, D., Tsai, Y.I. (2021). Brown carbon light absorption over an urban environment in northern peninsular Southeast Asia. Environ. Pollut. 276, 116735. https://doi.org/10.1016/j.envpol.2021.116735

Phairuang, W., Suwattiga, P., Chetiyanukornkul, T., Hongtieab, S., Limpaseni, W., Ikemori, F., Hata M., Furuuchi, M. (2019). The influence of the open burning of agricultural biomass and forest fires in Thailand on the carbonaceous components in size-fractionated particles. Environ. Pollut. 247, 238–247. https://doi.org/10.1016/j.envpol.2019.01.001

Pongpiachan, S., Ho, K.F., Cao, J. (2013). Estimation of gas-particle partitioning coefficients (Kp) of carcinogenic polycyclic aromatic hydrocarbons in carbonaceous aerosols collected at Chiang-Mai, Bangkok and Hat-Yai, Thailand. Asian Pac. J. Cancer Prev. 14, 2461–2476. https://doi.org/10.7314/apjcp.2013.14.4.2461

Pongpiachan, S., Ho, K., Cao, J. (2014a). Effects of biomass and agricultural waste burnings on diurnal variation and vertical distribution of OC/EC in Hat-Yai City, Thailand. Asian J. Appl. Sci. 7, 360–374. https://doi.org/10.3923/ajaps.2014.360.374

Pongpiachan, S., Kudo, S., Sekiguchi, K. (2014b). Chemical characterization of carbonaceous PM_{10} in Bangkok, Thailand Asian. J. Appl. Sci. 7, 325–342. https://doi.org/10.3923/ajaps.2014.325.342

Pongpiachan, S., Kositanont, C., Palakun, J., Liu, S., Ho, K.F., Cao, J. (2015). Effects of day-of week trends and vehicle types on $PM_{2.5}$-bounded carbonaceous compositions. Sci. Total Environ. 532, 484–494. https://doi.org/10.1016/j.scitotenv.2015.06.046

Pongpiachan, S., Hattayanone, M., Cao, J. (2017) Effect of agricultural waste burning season on $PM_{2.5}$-bound polycyclic aromatic hydrocarbon (PAH) levels in Northern Thailand. Atmos. Pollut. Res. 8, 1069–1080. https://doi.org/10.1016/j.apr.2017.04.009

Potter, N.A., Meltzer, G.Y., Avenbuan, O.N., Raja, A., Zelikoff, J.T. (2021). Particulate matter and associated metals: A link with neurotoxicity and mental health. Atmosphere 12, 425. https://doi.org/10.3390/atmos12040425

Ramirez, O., Campaa, A.M., Rosa, J. (2018). Characteristics and temporal variations of organic and elemental carbon aerosols in a high–altitude, tropical Latin American megacity. Atmos. Res. 210, 110–122. https://doi.org/10.1016/j.atmosres. 2018.04.006

Safai, P.D., Raju, M.P., Rao, P.S.P., Pandithurai, G. (2104). Characterization of carbonaceous aerosols over the urban tropical location and a new approach to evaluate their climatic importance. Atmos. Environ. 92, 493–500. https://doi.org/10.1016/j.atmosenv.2014.04.055

Schraufnagel, D.E. (2020). The health effects of ultrafine particles. Exp. Mol. Med. 52, 311–317. https://doi.org/10.1038/s12276-020-0403-3

Sharma, R., Balasubramanian, R. (2018). Size-fractionated particulate matter in indoor and outdoor environments during the 2015 haze in Singapore: Potential human health risk assessment. Aerosol Air Qual. Res. 18, 904–917. https://doi.org/10.4209/aaqr.2017.11.0515

Singh, R., Kulshrestha, M., Kumar, B., Chandra, S. (2016). Impact of anthropogenic emissions and open biomass burning on carbonaceous aerosols in urban and rural environments of Indo-Gangetic Plain. Air Qual. Atmos. Health 9, 809–822. https://doi.org/10.1007/s11869-015-0377-9

Sricharoenvech, P., Lai, A., Oo, T.N., Oo, M.M., Schauer, J.J., Oo, K.L., Aye, K.K. (2020). Source apportionment of coarse particulate matter (PM_{10}) in Yangon, Myanmar. Int. J. Environ. Res. Public Health 17, 4145. https://doi.org/10.3390/ijerph17114145

Tao, J., Surapipith, V., Han, Z., Prapamontol, T., Kawichai, S., Zhang, L., Zhang, Z., Wu, Y., Li, Jiawei, Li, Jie, Yang, Y., Zhang, R. (2020). High mass absorption efficiency of carbonaceous aerosols during the biomass burning season in Chiang Mai of northern Thailand. Atmos. Environ. 240, 117821. https://doi.org/10.1016/j. atmosenv.2020.117821

Tekasakul, P., Furuuchi, M., Tekasakul, S., Chomanee, J., Otani, Y. (2008). Characteristics of PAHs in particulates in atmospheric environment of the city of Hat Yai, Thailand and relation with rubber-wood burning in rubber sheet production. Aerosol Air Qual. Res. 8, 265–278. https://doi.org/10.4209/aaqr.2008.02.0004

Thepnuan, D., Chantara, S., Lee, C.T., Lin, N.H., Tsai, Y.I. (2019). Molecular markers for biomass burning associated with the characterization of $PM_{2.5}$ and component sources during dry season haze episodes in Upper South East Asia. Sci. Total Environ. 658, 708–722. https://doi.org/10.1016/j.scitotenv.2018.12.201

University of Wyoming (2021). Worldwide Radiosonde Soundings data. http://weather.uwyo.edu/upperair/sounding.html (accessed 26 January 2021).

Wiriya, W., Prapamontol, T., Chantara, S. (2013). PM_{10}-bound polycyclic aromatic hydrocarbons in Chiang Mai (Thailand): Seasonal variations, source identification, health risk assessment and their relationship to air-mss movement. Atmos. Res. 124, 109–122. https://doi.org/10.1016/j.atmosres.2012.12.014

Wiriya, W., Chantara, S., Sillapapiromsuk, S., Lin, N. (2016). Emission profiles of PM_{10}-bound polycyclic aromatic hydrocarbons from biomass burning determined in chamber for assessment

of air pollutants from open burning. Aerosol Air Qual. Res 16, 2716–2727. https://doi.org/10.4209/aaqr.2015.04.0278

Zhang, Y., Peng, Y., Song, W., Zhang, Y.L., Pongsawansong, P., Prapamontol, T., Wang, Y. (2021). Contribution of brown carbon to the light absorption and radiative effect of carbonaceous aerosols from biomass burning emissions in Chiang Mai, Thailand. Atmos. Environ. 260: 118544. https://doi.org/10.1016/j.atmosenv.2021.118544

Zhang, T., Cao, J.J., Chow, J.C., Shen, Z.X., Ho, K.F., Ho, S.S.H., Liu, S.X., Han, Y.M., Watson, J.G., Wang, G.H., Huang, R.J. (2014). Characterization and seasonal variations of levoglucosan in fine particulate matter in Xi'an, China. J. Air Waste Manage. Assoc. 64, 1317–1327. https://doi.org/10.1080/10962247.2014.944959

Zhu, C.S., Chen, C.C., Cao, J.J., Tsai, C.J., Chou Charles, C.K., Liu, S.C., Roam, G.D. (2010). Characterization of carbon fractions for atmospheric fine particles and nanoparticles in a highway tunnel. Atmos. Environ. 44, 2668–2673. https://doi.org/10.1016/j.atmosenv.2010.04.042